Transition Metal Oxide Supported on Alumina Catalysts: A Comparative Study for the Hydrogenation of Octanal

Jignesh Valand[†], Venkata D.B.C. Dasireddy, Abdul S. Mahomed iD **and
Holger B. Friedrich*** iD

*Catalysis Research Group, School of Chemistry and Physics, University of KwaZulu-Natal,
Private Bag X45001, Durban, 4000, South Africa.*

ABSTRACT

Monometallic (10 wt.%) Co, Ni and Cu nanoparticles supported on alumina catalysts were prepared using an ultrasonic impregnation-cavitation method and characterized using ICP, XRD, physisorption, chemisorption and temperature programmed techniques. The copper catalyst showed higher metal dispersion and greater hydrogen and CO chemisorption capacity when compared to the nickel and cobalt catalysts. Hydrogenation of octanal carried out in a continuous flow high pressure fixed bed reactor showed that the rate of reaction and turnover number of octanol depended on the amount of hydrogen chemisorbed. The copper catalyst showed the lowest activation energy, as well as best catalytic activity. The Cu-Al catalyst which showed higher metal dispersion and low acidity, showed the highest selectivity towards octanol with no C24 acetal formation, when compared to the Ni-Al and Co-Al catalysts.

1. Introduction

Linear α-olefins (LAOs) are an important feedstock for the chemical industry.[1] These compounds are produced from catalytic cracking, resulting in a large number of different types of 1-alkenes as the primary products, together with alkanes.[2] These valuable terminal alkenes are also produced by the dehydration of primary alcohols. These alcohols, in turn, can be prepared by the hydrogenation of carbonyl compounds formed, e.g. in the hydroformylation reaction.[3] Catalytic conversion of carbonyl compounds to alcohols is one of the more demanding reactions in organic synthesis and also is used in the production of fine chemicals.

From the early 1930s, triglycerides, primarily vegetable oils, have been transformed to fatty alcohols by hydrogenation over Cr-containing Adkins catalysts.[4] The use of chromium is known to cause concern regarding health and environmental issues, as a result the search for environmentally friendly and benign hydrogenation catalysts is continuing.[3,5] Reports on the selective hydrogenation of aldehydes to alcohols in continuous flow liquid phase systems, under mild conditions are limited.[6] There are reports on using group VIII metals on oxide supports for the hydrogenation of aldehydes.[3,7] Catalysts with metals such as nickel,[8] palladium[9] or rhodium[10] are not selective towards unsaturated alcohols, whereas ruthenium has moderate activity and similar or better selectivities are achieved with platinum, iridium or osmium catalysts.[11] Those metals, however, are rare and expensive.

It has been shown that hydrogenation depends on the surface area, pore volume and acid-base character of the support.[11–12] High surface area enhances dispersion of supported metals, whereas porosity of the support affects intraparticle diffusion of reactants and products. The acid-base nature of the support is a key parameter to allow or restrict the formation of acetals and diols in the hydrogenation of aldehydes.[1, 11a] Hydrogenation of a long chain aldehyde, e.g. octanal is one of the interesting topics of research in the field of catalysis. In the present study, we report the hydrogenation of 1-octanal to 1-octanol, an important step in an industrial process which ultimately gives 1-octene, over the comparatively inexpensive transition metals cobalt, nickel and copper supported on alumina, prepared by an ultrasonication process.

2. Experimental

The ultrasonic cavitation-impregnation method[13] was used for preparing the supported catalysts. These materials were made by dissolving the required amounts of the metal precursors, cobalt nitrate ($Cu(NO_3)_2 \cdot 3H_2O$, Sigma-Aldrich), nickel nitrate ($Ni(NO_3)_2 \cdot 6H_2O$, Sigma-Aldrich), and copper nitrate ($Co(NO_3)_2 \cdot 6H_2O$, ACE) in distilled water, then adding the solutions to high surface area λ-alumina (λ-Al_2O_3, Alfa-Aesar). Magnetic stirring at 300 rpm, combined with ultrasonic cavitation (MRC Ultrasonic System, D150H Model) at 43 kHz were applied at room temperature (25 ± 1 °C) to obtain a homogeneous mixture and uniform dispersion. The slurry was dried by evaporation at 70 °C while stirring continuously. The materials then were dried in an oven for 16 h at 110 °C. The catalysts then were calcined for 5 h at 550 °C to give the 10 wt.% of cobalt, nickel and copper catalysts, denoted as Cu-Al, Ni-Al and Co-Al, respectively.

The Brunauer-Emmett-Teller (BET) surface area was measured using a Micromeritics Tristar II instrument. Inductively coupled plasma (ICP) analyses were carried out with a Perkin Elmer Optical Emission Spectrometer Optima 5300 DV. Powder X-ray diffraction (XRD) was conducted using a Bruker D8 Advance

[†]Present address: Department of Materials Science, Sardar Patel University, Vallabh Vidyanagar-388120, Gujarat, India.

* To whom correspondence should be addressed. E-mail: friedric@ukzn.ac.za

diffractometer equipped with a Cu radiation source (λ = 1.5406 Å). NH_3-temperature programmed desorption (NH_3-TPD) was done on a Micromeritics 2920 Autochem II Chemisorption Analyser. In these analyses a mixture of 5 % NH_3 in helium was passed over the reduced catalyst for 60 min. Thereafter, the temperature was increased slowly to 950 °C by ramping at 10 °C min^{-1} under helium flow.[14] The dispersion of metals, crystallite size, hydrogen and CO uptake were determined with the use of a Micromeritics ASAP 2020 Chemisorption Analyser. The metal dispersion is expressed as the ratio between hydrogen uptake and the metal on the surface of the support. It was calculated assuming a 1:1 H:M (M = Co, Ni and Cu) chemisorption stoichiometry.[3] The equations used to establish dispersion and metal surface area can be found in the supplementary information. A Jeol JEM-1010 electron microscope was used to obtain TEM images of the catalysts.

The hydrogenation reactions were performed in a fixed bed continuous flow reactor in down-flow mode. The catalyst bed (4 mL volume, pellet sizes ranged between 300 and 600 μm) was diluted with an equal volume of carborundum (24 grit). Prior to the catalytic testing, to ensure that the reactor is free from physical transport limitations, the reactor set-up was checked with varying flows of octanal, pressures and pellet sizes of catalysts. The feed used for all reactions was 10 wt.% octanal in octanol, the latter serving as thermal diluent. Octanol does not affect the reaction. There was no decrease in octanal conversion with increasing dilution, which shows the absence of diluent effects during the reaction.[15] The feed entered the reactor *via* a Lab Alliance Series II hplc pump. The liquid products were collected in a 500 mL catchpot and the excess hydrogen gas exited through a wet gas flow meter (Ritter Drum-type). The liquid products were collected at regular intervals. They were identified and quantified using a PerkinElmer Clarus 500 GC, with an FID and a Petrolite column. All the reported data points were obtained in duplicate after steady state was achieved. The mass balances for all samples were 100 ± 1 %.

TON, also called turnover number, was defined as the molecules reacting per active site per gram of catalyst. The number of reacting molecules of octanal was calculated using the conversion and mass flow rate data at corresponding reaction temperatures; and the available number of active sites was obtained from the metal dispersion data, measured from chemisorption. The apparent activation energy was calculated using the Arrhenius plot, details of which are found in the supplementary information.

3. Results and Discussion

3.1. Characterisation of the Catalysts

Table 1 shows the results of the physisorption experiments and the elemental analyses of the catalysts. The ICP data of the catalysts showed that the desired metal wt.% was loaded on the alumina. All the catalysts show Type IV adsorption desorption isotherms with a H1 hysteresis loop, which demonstrated the

mesoporous nature of the catalysts.[14] By impregnating the metal oxides on alumina, the surface area and pore volume decreased, likely due to the blocking of the narrow pores of alumina with the metal oxides. Powder XRD (Fig. 1) shows the alumina pattern which is in agreement with the literature[2] and with JCPDS File No. 10-425. The d-spacing values for the 2θ angles between 30 ° to 50 ° correlate with the JCPDS File Nos. 41-254, 47-1049, 42-1467 for copper oxide, nickel oxide and cobalt oxide, respectively.[4b] Among all the catalysts, Co-Al showed the largest crystallite size compared to Cu-Al and Ni-Al (Table 2). In general, the larger crystallite size of the metals leads to lower dispersion of the metal on the surface of the support.[15c] The same trend is observed in this study. The amount of hydrogen chemisorbed on the surface of the catalysts was in the inverse order to crystallite size.

In the TPD analysis data, all catalysts showed three types of acidic sites, i.e. weak (<400 °C), moderate (400–600 °C) and strong (600–900 °C).[2] In all the catalysts, weak acidic sites are dominant and Co-Al showed the highest Lewis acidity, whereas Ni-Al showed the highest total and specific acidity (Table 3). Cu-Al showed the lowest acidity when compared to other catalysts, but slighter higher acidity than the alumina support. In the TEM images (Fig. S1, supplementary information), alumina appears as irregular-shaped agglomerations of elongated particles. When the Cu, Ni and Co oxides were impregnated, no difference in the overall morphology of the catalysts was observed.

3.2. Catalytic Results

The hydrogenation of octanal was conducted in a continuous flow fixed bed reactor with an octanal to hydrogen molar ratio of 1:2. GHSV and LHSV were maintained at 460 h^{-1} and 18 h^{-1}, respectively, at temperatures of 110 °C, 150 °C and 180 °C. With an increase in temperature, all the catalysts showed the expected increase in conversion of octanal and also an increased selectivity towards octanol.

Figure 2 shows the conversion of octanal and selectivity towards products at 110 °C. The conversion profile of the catalysts correlates with the amount of hydrogen chemisorbed on the surface of the catalysts (Table 2), which suggests the conversion of the octanal depends on the disassociation of hydrogen on the surface of the catalyst.[16] The copper-containing catalyst is significantly more active than other catalysts, due to high metal dispersion and acidic site distribution (Fig. 2). The selectivity profile of octanol is proportional to the quantity of CO chemisorbed on the surface of the catalysts in chemisorption studies, which might imply a correlation with carbonyl group (octanal) adsorption.

The desired reaction in this study is the hydrogenation of octanal to produce octanol. However, some side reactions do occur to produce the C16 diol and C24 acetal. The C16 diol is produced over the Cu-Al catalyst and occurs through an acid-base catalyzed aldol condensation of two octanal molecules to form the C16 aldol, which is further hydrogenated to form the

Table 1 Summary of physisorption and elemental analysis.

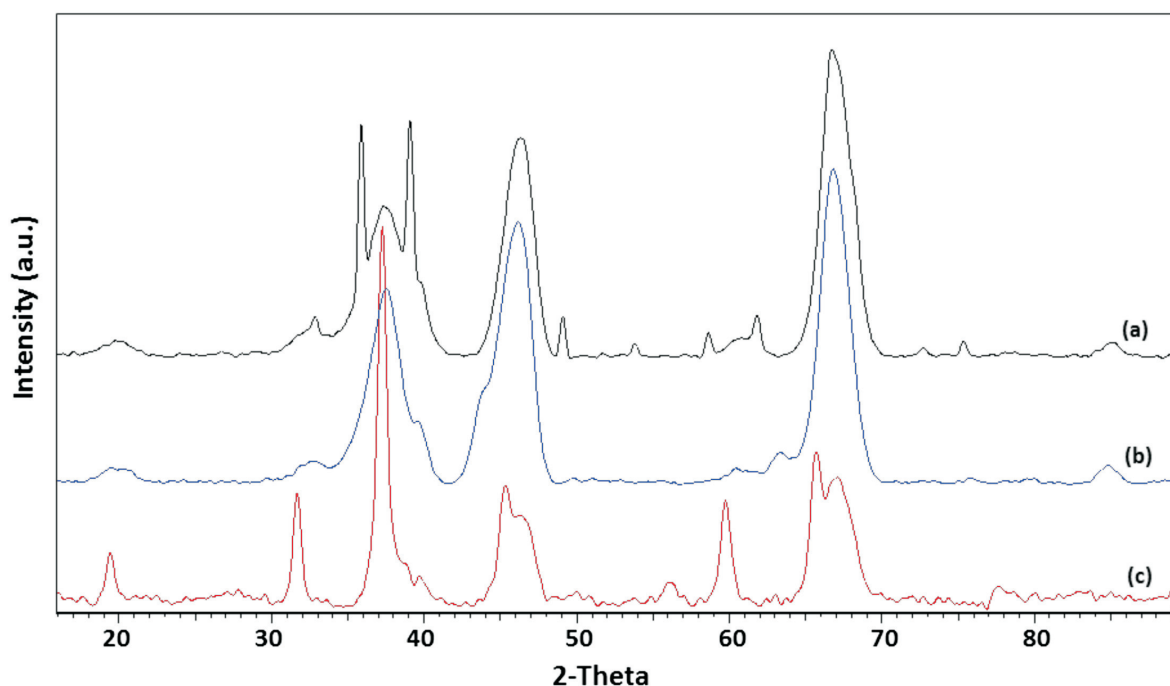| Sample code	BET surface area /m^{2}g^{-1}	Total pore volume /cm^3 g^{-1}	Average pore size /nm	Metal loadings /wt.%
γ-Alumina	263	0.84	12.8	–
Cu-Al	193	0.63	12.4	9.6
Ni-Al	201	0.69	12.0	9.8
Co-Al	197	0.62	12.3	9.9

Figure 1 Powder XRD patterns of (a) Cu-Al (b) Ni-Al and (c) Co-A1 catalysts.

C16 diol.[17] The C24 acetal formation is mainly an acid catalyzed reaction and is produced by the Ni-Al and Co-Al catalysts, which showed relatively high specific acidity. Here, the reaction between octanal and octanol tales place over the acidic sites to form C16 hemi acetals which upon dehydration with octanol produces the C24 acetal. The C24 acetal selectivity decreased with increase in temperature. In addition to octanol, C24 acetal and C16 diols, other products (2-hexyl decanol, octanoic acid, octyloctanoate) also formed in small quantities.

Figure 3 shows the product selectivity at an iso-conversion of 95 %, at a temperature of 150 °C and an octanal to hydrogen molar ratio of 2. The product selectivity at iso-conversion is influenced by the metal dispersion and acidic site distribution of the catalysts. The Cu-Al catalyst which showed higher metal dispersion and low acidity, showed the highest selectivity towards octanol with no C24 acetal formation, when compared

to the Ni-Al and Co-Al catalysts. No significant difference is seen in the selectivities towards products for the Ni-Al and Co-Al catalysts, probably due to their similar specific acidities and high acidity when compared to the Cu-Al catalyst.

3.3. Kinetics of the Reaction

To gain insight into the reaction mechanism in this study, the rate of the reaction of octanal hydrogenation and turnover number toward octanol were calculated. Since all reactions were carried out at 50 bar pressure, it is assumed that there would be no mass transfer limitations of gaseous hydrogen to the liquid phase. It was also assumed that adsorbed hydrogen was effectively at equilibrium and that the rate limiting step of the reaction is the addition of the second hydrogen atom to the organic moiety.[15] As a result, the rate expression was determined to be first order in both aldehyde concentration and hydrogen partial

Table 2 Summary of the chemisorption analysis.

Sample code	Metal dispersion /%	Metallic surface area /$m^2 g^{-1}$ *	Crystallite size /nm	Amount of H_2 chemisorbed /$cm^3 g^{-1}$ #	Amount of CO chemisorbed $cm^3 g^{-1}$ #
Cu-Al	6.0	3.7	1.8	0.018	0.058
Ni-Al	5.2	3.4	2.2	0.016	0.032
Co-Al	1.3	0.9	7.5	0.011	0.045

* From the Debye-Scherrer equation; # measured at a pressure of 350 mmHg

Table 3 NH_3-TPD data of the prepared catalysts.

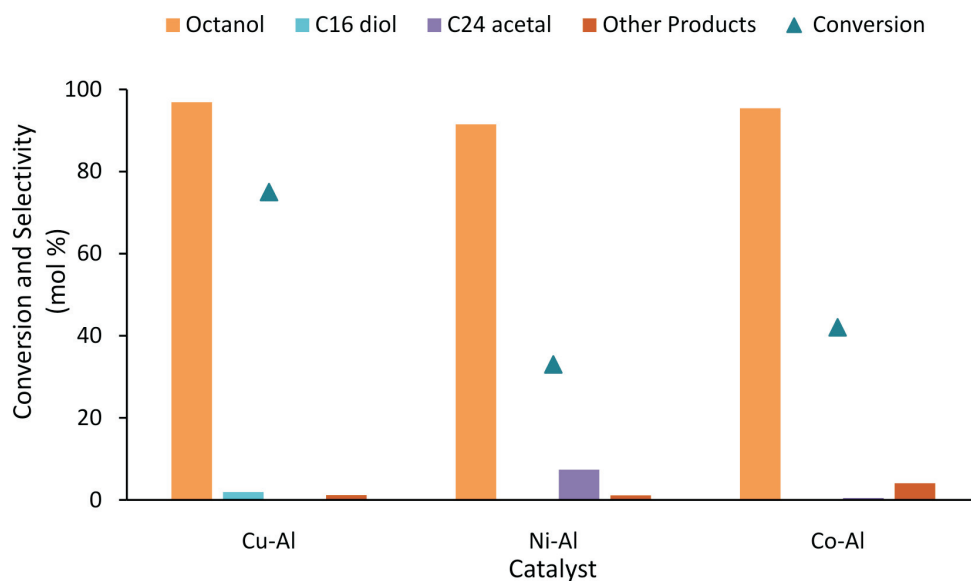| Sample code	Acidity /mmol NH_3 g^{-1}			Total acidity /mmol NH_3 g^{-1}	Specific acidity /mmol NH_3 m^{-2}
	Weak (<400 °C)	Moderate (400–600 °C)	Strong (600–900 °C)		
Alumina	159	57	2	218	0.82
Cu-Al	168	63	12	243	1.25
Ni-Al	174	81	16	271	1.34
Co-Al	171	72	14	257	1.30

Figure 2 Catalytic activity of octanal hydrogenation at 110 °C. The molar ratio of octanal to hydrogen is 2 and the LHSV is 18 h^{-1}.
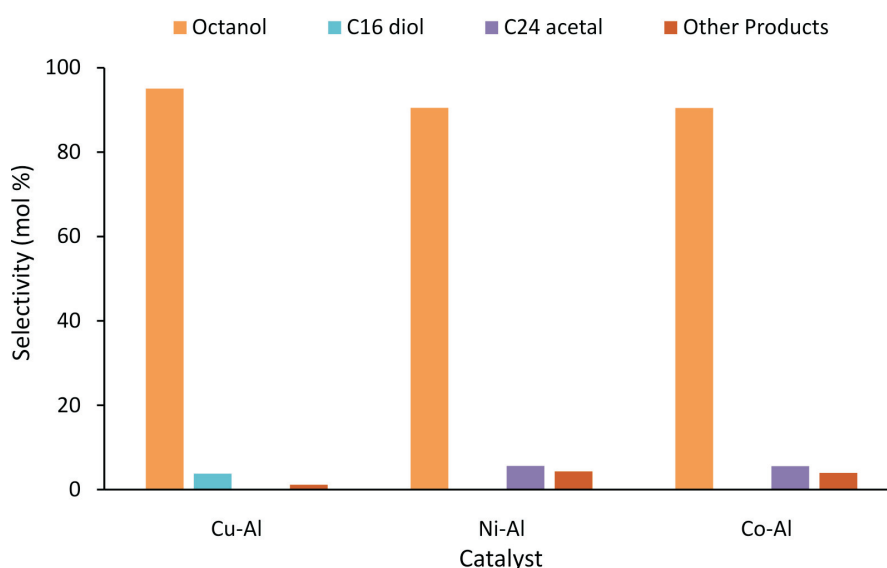

Figure 3 Product selectivity at iso-conversion (95 %) at 150 °C. The octanal to hydrogen molar ratio is 2.

pressure.[1,6] The rate of the reaction of catalytic hydrogenation of octanal was found to be proportional to the metal dispersion of the catalysts (Table 4). The catalyst with highest metal dispersion and lowest acidity, i.e Cu-Al, showed the highest rate and the lowest activation energy. The turnover number toward octanol was greater over the Cu-Al catalyst, than over both the Ni-Al and Co-Al catalysts.

Table 4 Kinetic data of hydrogenation reactions.

Sample code	Rate of reaction /10^{-2} s^{-1}	Turn over number /mol g^{-1}	Activation energy /kJ mol^{-1}
Cu-Al	6.9	29.4	2.2
Ni-Al	3.8	20.8	4.3
Co-Al	2.9	21.3	6.1

4. Conclusion

All three catalysts showed good catalytic hydrogenation activity, however, the Cu-Al catalyst performed better when compared to the Ni-Al and Co-Al catalysts. Cu-Al showed the highest metal dispersion, whereas Co-Al showed the lowest

metal dispersion which directly affects the catalyst performance under hydrogenation. Octanal conversion was dependent on the dispersion of metal on the catalysts. The selectivity profiles match the acidic site distributions of the catalysts at iso-conversion. In addition to octanol, other products such as the C16 diol and the C24 acetal were observed in small amounts, which formed *via* acid-base catalysis on the surface. Octanal hydrogenation follows first-order kinetics and the rate of the reaction is also dependent on the metal dispersion of the catalysts. Among all the catalysts, Cu-Al showed the lowest activation energy and thus highest activity.

Supplementary Material

Supplementary information is provided in the online supplement.

§**ORCID iDs**

A.S. Mahomed: orcid.org/0000-0002-1255-5500
H.B. Friedrich: orcid.org/0000-0002-1329-0815

References

1 H. Hattori, Heterogeneous basic catalysis, *Chem. Rev.*, 1995, **95**, 537–558.

2 H. F. Rase, *Handbook of Commercial Catalysts: Heterogeneous Catalysts*, Taylor & Francis, 2000.

3 K. Ralphs, C. Hardacre and S.L. James, Application of heterogeneous catalysts prepared by mechanochemical synthesis, *Chem. Soc. Rev.*, 2013, **42**, 7701–7718; b) T. Chetty, V.D.B.C. Dasireddy, L.H. Callanan and H.B. Friedrich, Continuous flow preferential hydrogenation of an octanal/octene mixture using Cu/Al$_2$O$_3$ catalysts, *ACS Omega*, 2018, **3**, 7911–7924.

4 a) A. Vaccari, Clays and catalysis: a promising future, *Appl. Clay Sci.*, 1999, **14**, 161–198; b) W. Huang, H. Li, B. Zhu, Y. Feng, S. Wang and S. Zhang, Selective hydrogenation of furfural to furfuryl alcohol over catalysts prepared via sonochemistry, *Ultrasonics Sonochemistry*, 2007, **14**, 67–74.

5 Y. Li, Q. Fu and M. Flytzani-Stephanopoulos, Low-temperature water-gas shift reaction over Cu- and Ni-loaded cerium oxide catalysts, *Appl. Catal. B: Environ.*, 2000, **27**, 179–191.

6 a) A. Corma and M.J. Sabater, in *Environmental Catalysis over Gold-Based Materials*, The Royal Society of Chemistry, 2013, pp. 146–200; b) P. Gallezot and D. Richard, Selective hydrogenation of α, β-unsaturated aldehydes, *Catal. Rev.*, 1998, **40**, 81–126.

7 a) F. Studt, F. Abild-Pedersen, Q. Wu, A.D. Jensen, B. Temel, J.-D. Grunwaldt and J.K. Nørskov, CO hydrogenation to methanol on Cu–Ni catalysts: theory and experiment, *J. Catal.*, 2012, **293**, 51–60; b) G.J. Hutchings, F. King, I.P. Okoye and C.H. Rochester, Influence of chlorine poisoning of copper/alumina catalyst on the selective hydrogenation of crotonaldehyde, *Catal. Lett.*, 1994, **23**, 127–133; c) V. Gutierrez, M. Dennehy, A. Diez and M.A. Volpe, Liquid phase hydrogenation of crotonaldehyde over copper incorporated in MCM-48, *Appl. Catal. A: Gen.*, 2012, **437–438**, 72–78.

8 J. Zhang, H. Wang and A.K. Dalai, Effects of metal content on activity and stability of Ni-Co bimetallic catalysts for CO$_2$ reforming of CH$_4$, *Appl. Catal. A: Gen.*, 2008, **339**, 121–129.

9 F. Coloma, A. Sepúlveda-Escribano, J.L.G. Fierro and F. Rodríguez-Reinoso, Gas phase hydrogenation of crotonaldehyde over Pt/activated carbon catalysts. Influence of the oxygen surface groups on the support, *Appl. Catal. A: Gen.*, 1997, **150**, 165–183.

10 C. Ando, H. Kurokawa and H. Miura, Selective hydrogenation of aldehyde groups in various α, β-unsaturated aldehydes over alumina-supported cobalt(0) catalyst, *Appl. Catal. A: Gen.*, 1999, **185**, L181–L183.

11 a) M. Sankar, N. Dimitratos, P.J. Miedziak, P.P. Wells, C.J. Kiely and G.J. Hutchings, Designing bimetallic catalysts for a green and sustainable future, *Chem. Soc. Rev.*, 2012, **41**, 8099–8139; b) G. Li, P. Dong, D. Ji, Y. Xu, Y. Li and R. Mu, Effect of support materials on liquid-phase hydrogenation of hydroquinone over ruthenium catalysts, *Solid State Sci.*, 2013, **23**, 13–16.

12 a) K. Chen, S. Xie, A.T. Bell and E. Iglesia, Structure and properties of oxidative dehydrogenation catalysts based on MoO$_3$/Al$_2$O$_3$, *J. Catal.*, 2001, **198**, 232–242; b) J. Xue, F. Cui, Z. Huang, J. Zuo, J. Chen and C. Xia, Effect of metal additives on structure and properties of a Co/SiO2 hydrogenation catalyst, *Chin. J. Catal.*, 2012, **33**, 1642–1649; c) P. López, Mondragón-Galicia, M.E. Espinosa-Pesqueira, D. Mendoza-Anaya, M.E. Fernández, A. Gómez-Cortés, J. Bonifacio, G. Martínez-Barrera and R. Pérez-Hernández, Hydrogen production from oxidative steam reforming of methanol: effect of the Cu and Ni impregnation on ZrO$_2$ and their molecular simulation studies, *Int. J. Hydrogen Energy*, 2012, **37**, 9018–9027.

13 J.H. Bang and K.S. Suslick, Applications of ultrasound to the synthesis of nanostructured materials, *Adv. Mater.*, 2010, **22**, 1039–1059.

14 C.A. Brebbia and A. Klemm, *Materials Characterisation VI: Computational Methods and Experiments*, WIT Press, 2013.

15 a) T. Chetty, H.B. Friedrich, V.D.B.C. Dasireddy, A. Govender, P.J. Mohlala and W. Barnard, Effect of various Au/Al$_2$O$_3$ preparations on catalytic behaviour during the continuous flow hydrogenation of an octanal/octene mixture, *ChemCatChem*, 2014, **6**, 2384–2393; b) S.F. Miller, H.B. Friedrich, C.W. Holzapfel and V.D.B.C. Dasireddy, Effects of organic modifiers on a palladium catalyst in the competitive hydrogenation of 1-octene versus octanal: an evaluation of solid catalysts with an ionic liquid layer, *ChemCatChem*, 2015, **7**, 2628–2636; c) J. Valand, V.D.B.C. Dasireddy, S. Singh and H.B. Friedrich, Ternary (Cu, Ni and Co) nanocatalysts for hydrogenation of octanal to octanol: an insight into the cooperative effect, *Catal. Lett.*, 2017, **147**, 525–538.

16 L. Cervený, *Catalytic Hydrogenation*, Elsevier Science, 1986.

17 a) J. Valand, A.S. Mahomed, S. Singh and H.B. Friedrich, The influence of Montmorillonite K10 as a support in the nickel catalyzed hydrogenation of octanal, *J. Porous Mat.*, 2016, **23**, 175–183; b) M.D. Farahani, J. Valand, A.S. Mahomed and H.B. Friedrich, A comparative study of NiO/Al$_2$O$_3$ catalysts prepared by different combustion techniques for octanal hydrogenation, *Catal. Lett.*, 2016, **146**, 2441–2449.

<div align="center">**Supplementary Data**</div>

Chemisorption analysis (Micromeritics ASAP 2020):

Metal dispersion (%):

$$\% \, M_{disp} = \frac{100\% \times 100\%}{22414^*} \times \frac{V \times SFcalc}{\%Weight / Watomic}$$

Where,

$\%M_{DISP}$ is metal dispersion (%)

V in cm^3/g, STP, is volume intercept derived from the best line fit to the volume differences between the selected points of the first analysis and the repeat analysis. If $\%M_{Disp}$ is being calculated from analysis data, then V is the volume intercept derived from the best line fit of the points selected for line fit. If $M\%_{Disp}$ is being calculated from difference data, then V is V_{Diff}.

SF_{Calc} is the calculated stoichiometry factor

The calculated stoichiometry factor is a weighted average. It is dependent on both the individual stoichiometry factor and the number of moles of each active metal

%Weight is % of sample weight for metal

W_{Atomic} is atomic weight of metal (g/mole)

Metallic surface area:

The metallic surface area per gram of sample is the total active surface area available for interaction with the adsorbate and is calculated using the equation;

$$M_{sa} = \frac{6.023 \times 10^{23}}{22414^*} \times V \times SF_{CALC} \times A_{AREA}$$
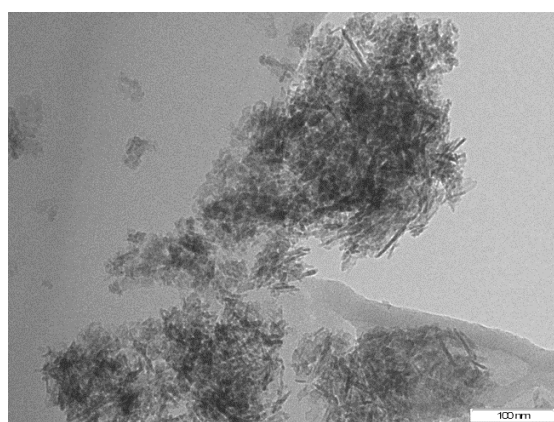
Where,

M_{sa} is the metallic surface area (m^2/g) of sample

V = (cm^3/g STP). If M_{sa} is being calculated from analysis data, then V is the volume intercept derived from the best line fit of the points selected for line fit. If M_{sa} is being calculated from difference data, then V is V_{Diff}.
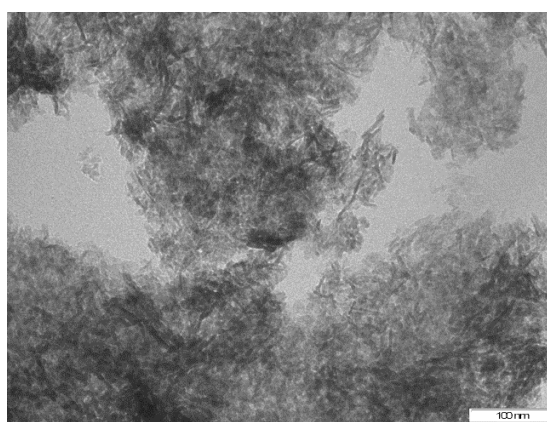
A_{AREA} is effective area of 1 active metal atom (m^2/atom)

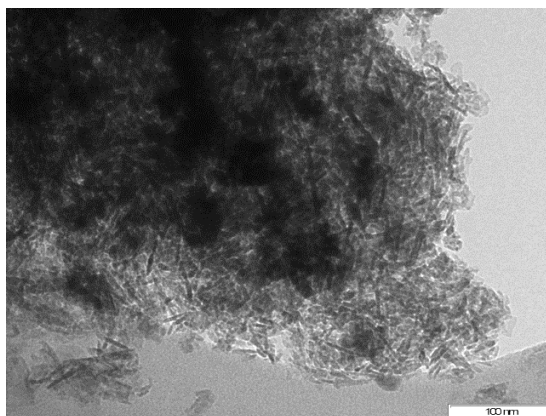SF_{CALC} is the calculated stoichiometry factor

V_{DIFF} is difference in volume between the first analysis and the repeat analysis

(a)

(b)

(c)

Fig. S1. TEM images of (a) Cu-Al (b) Ni-Al and (c) Co-A1 catalysts.

Activation energy:

The Activation Energy (Ea) was calculated using the Arrhenius Equation:

$$k = Ze^{-E_a/RT}$$

Where Z (or A) is the pre-exponential factor, k is the rate constant, R is the gas constant (8.314 J/mol-K), T is the temperature in Kelvin. When lnk (rate constant) is plotted against the inverse of the temperature (kelvin), the slope is a straight line. The value of the slope (m) is equal to -E_a/R where R is a constant equal to 8.314 J/mol-K. Z or A was determined from the intercept.

The activation energy in this study was calculated by using the rate constant (assuming first order reaction), calculated by the conversion of octanal obtained with an octanal to hydrogen molar ratio of 1:2. GHSV and LHSV were maintained at 460 h^{-1} and 18 h^{-1} respectively, at temperatures of 110 ºC, 150 ºC and 180 ºC.

Turn over number (TON):

Turn over number = (moles of octanal converted)/(moles of active sites per gram of catalyst) or mol g^{-1} .